Entangled-photon compressive ghost imaging

Petros Zerom,[1] Kam Wai Clifford Chan,[2] John C. Howell,[3] and Robert W. Boyd[1,3,4]

[1]*Institute of Optics, University of Rochester, Rochester, New York 14627, USA*
[2]*Rochester Optical Manufacturing Company, 1260 Lyell Avenue, Rochester, New York 14606, USA*
[3]*Department of Physics and Astronomy, University of Rochester, 500 Wilson Boulevard, Rochester, New York 14627, USA*
[4]*Department of Physics, University of Ottawa, Ottawa, Ontario, Canada K1N 6N5*

We have experimentally demonstrated high-resolution compressive ghost imaging at the single-photon level using entangled photons produced by a spontaneous parametric down-conversion source and using single-pixel detectors. For a given mean-squared error, the number of photons needed to reconstruct a two-dimensional image is found to be much smaller than that in quantum ghost imaging experiments employing a raster scan. This procedure not only shortens the data acquisition time, but also suggests a more economical use of photons for low-light-level and quantum image formation.

PACS number(s): 42.65.Lm, 42.30.Va, 42.30.Wb

Introduction. A key goal of many imaging protocols is to form an image using as small a number of photons as possible. Such strategies are especially useful for applications in quantum information, where the quantum nature of the light field is a key aspect of the problem at hand, or in other applications where photons are "expensive," such as in image formation at unusual wavelengths. In this Rapid Communication, we show that compressive sensing, which is also known as compressive sampling (CS), can be usefully implemented at the level of few-photon imaging.

CS is a novel sampling and signal reconstruction method that requires far less data than would be deemed necessary by the Nyquist-Shannon criterion [1–3]. As a resource-efficient sensing paradigm, CS has proven to be extremely useful in the context of classical image formation. The method has also been applied to quantum state tomography [4] and quantum process tomography [5], but has not to our knowledge previously been implemented in the context of quantum imaging. One can anticipate its importance in such a context, where a primary goal is to transfer an image using the absolute minimum number of transmitted photons.

Quantum imaging with entangled photons suffers from low photon flux and resource-inefficient transverse detection. These problems are strongly coupled. Owing to the need for gating to achieve high temporal resolution, transverse arrays are expensive and require intensive electronics even for low- to moderate-resolution images. A cheaper and simpler method is to raster scan a single-element detector to acquire the image. However, to obtain images with high resolution and high signal-to-noise ratio, long integration times are required.

In the present paper, we demonstrate the utility of CS in the context of a specific quantum imaging protocol, that of single-photon ghost imaging. The success of this demonstration suggests that CS methods are likely to prove useful much more generally in applications involving quantum light fields.

The configuration of the classical single-pixel camera [6] is conceptually equivalent to that of computational ghost imaging [7,8]. Conventionally, a ghost imaging (quantum or thermal) setup involves two beams of light, which are termed object and reference beams [9–14]. The object beam illuminates the object and the transmitted or reflected light is monitored by a spatially nonresolving (bucket) detector. The light in the reference arm is monitored by a spatially resolving detector. The image of the object (the so-called ghost image) is then formed by a coincidence measurement (in the quantum case) or intensity correlation (for the thermal case) between the object and reference signals. In computational ghost imaging [7,8] and in compressive thermal ghost imaging [15], a single-beam and a single spatially nonresolving detector are used. In both cases, the intensity distribution of the reference beam is determined computationally.

Here we demonstrate experimentally the operation of quantum compressive ghost imaging at the single-photon level using biphotons generated by spontaneous parametric down-conversion (SPDC). We find in our experiment that for a given mean-squared error of the reconstructed quantum ghost image, the number of measurements (and the number of photons) needed by the CS algorithm is much smaller than that using a raster scan. This finding not only implies an improvement in acquisition time, but also suggests a more economical use of photons for low-light-level imaging.

Theory. Our theoretical analysis and experiments focus on quantum compressive ghost imaging using photons generated by SPDC. Nevertheless, it is instructive to compare our configuration with the single-photon compressive imaging setup depicted in Fig. 1(a). The figure shows a single-pixel camera with the object being illuminated by heralded single photons produced by SPDC. Because of the use of entangled photons as the light source, the setup can be recast into a ghost imaging configuration as shown in Fig. 1(b). One can see the similarity of the two setups through use of Klyshko picture [9] diagrams (see the insets). Note that in either case the object is imaged onto the spatial light modulator (SLM).

The coincidence count signal for the detectors at $\mathbf{x}_1$ and $\mathbf{x}_2$ is proportional to the normally ordered correlation function [16,17]

$$C(\mathbf{x}_1,\mathbf{x}_2) = \langle\psi|\,\hat{E}^{(-)}(\mathbf{x}_1)\hat{E}^{(-)}(\mathbf{x}_2)\hat{E}^{(+)}(\mathbf{x}_2)\hat{E}^{(+)}(\mathbf{x}_1)\,|\psi\rangle$$
$$= |\langle 0|\hat{E}^{(+)}(\mathbf{x}_1)\hat{E}^{(+)}(\mathbf{x}_2)|\psi\rangle|^2, \qquad (1)$$

where $\hat{E}^{(+)}(\mathbf{x})$ and $\hat{E}^{(-)}(\mathbf{x})$ are the positive- and negative-frequency part of the electric-field operator at position $\mathbf{x}$ and $|\psi\rangle$ is the biphoton state. Unlike previous ghost imaging configurations [9–13,18] in which a spatially
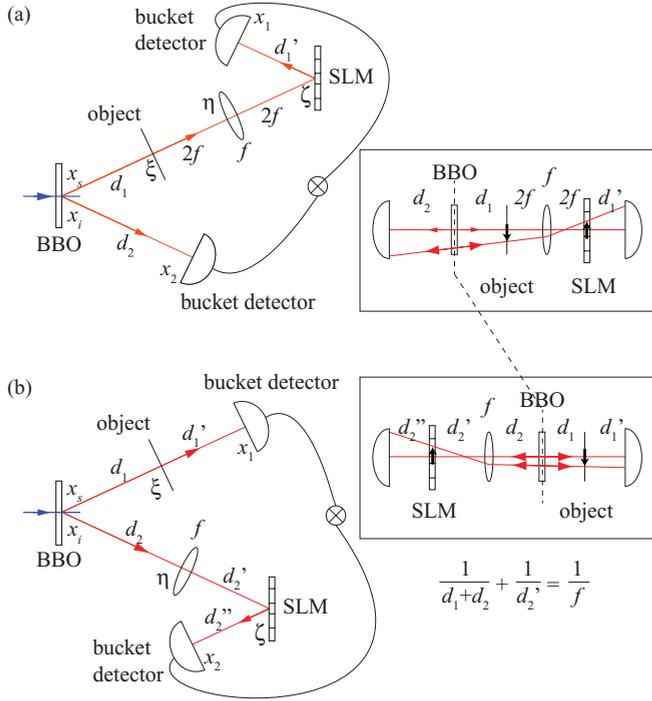
(a)

(b)

FIG. 1. (Color online) Schematics for (a) compressive single-photon imaging and (b) compressive quantum ghost imaging. Insets: the corresponding Klyshko pictures.

resolving detector is used in the reference arm, bucket detectors are used in both arms in our case. All the object information is thus contained in the integrated coincidence signal $C_m = \int d\mathbf{x}_1 \, d\mathbf{x}_2 \, C(\mathbf{x}_1, \mathbf{x}_2)$, where m denotes the mth measurement, as we describe in detail below. For the setup of Fig. 1(b), the two-photon amplitude is given by

$$
\begin{aligned}
&\langle 0|\hat{E}^{(+)}(\mathbf{x}_2)\hat{E}^{(+)}(\mathbf{x}_1)|\psi\rangle \\
&= \int d\mathbf{x}_s \, d\boldsymbol{\xi} \, d\boldsymbol{\eta} \, d\boldsymbol{\zeta} \, d\mathbf{x}_i \, h(\mathbf{x}_2,\boldsymbol{\zeta}) \, A_m(\boldsymbol{\zeta}) \, h(\boldsymbol{\zeta},\boldsymbol{\eta}) \, L(\boldsymbol{\eta}) \\
&\quad \times h(\boldsymbol{\eta},\mathbf{x}_i) \, \psi(\mathbf{x}_s,\mathbf{x}_i) \, h(\boldsymbol{\xi},\mathbf{x}_s) \, T(\boldsymbol{\xi}) \, h(\mathbf{x}_1,\boldsymbol{\xi}), \quad (2)
\end{aligned}
$$

where $h(\mathbf{x},\mathbf{x}') \propto \exp[ik/(2d)(\mathbf{x}-\mathbf{x}')^2]$ is the paraxial Fresnel free-space propagation kernel and $L(\mathbf{x}) = \exp[-ik/(2f)\,\mathbf{x}^2]$ is the transfer function of the lens. Here f is the focal length of the lens, d is the longitudinal separation between the $\mathbf{x}$ and $\mathbf{x}'$ planes, and $k = 2\pi/\lambda$ is the wave number. $T(\mathbf{x})$ is the transmission function of the object and is the quantity we wish to determine, and $A_m(\mathbf{x})$ is the two-dimensional random pattern imprinted onto the SLM with $m = 1,\ldots,M$, where M is the total number of realizations. The random patterns $A_m(x)$ used in conjunction with the bucket detector map the spatial information contained in the object function $T(x)$ into a sequence of coincidence signals encoded by the different realizations of A_m.

The biphoton state in the SPDC process can be approximated by $\psi(\mathbf{x}_s,\mathbf{x}_i) \propto \delta(\mathbf{x}_s - \mathbf{x}_i)$ for a thin nonlinear crystal and narrow bandpass filters before the detectors [19]. Under such conditions (which are good approximations in our experiment and many experiments on ghost imaging) and when the thin lens equation $1/(d_1 + d_2) + 1/d_2' = 1/f$ is satisfied, the

integrated coincidence signal becomes

$$
\begin{aligned}
C_m &= \int d\mathbf{x}_1 d\mathbf{x}_2 |\langle 0|\hat{E}^{(+)}(\mathbf{x}_1)\hat{E}^{(+)}(\mathbf{x}_2)|\psi\rangle|^2 \\
&\propto \sum_n |A_m(-\boldsymbol{\xi}_n)|^2 |T(\boldsymbol{\xi}_n)|^2, \quad (3)
\end{aligned}
$$

in which unit magnification of the imaging lens and the finite size of the SLM pixel are used, with $n = 1,\ldots,N$, where N is the number of pixels in the SLM. Note that the object and SLM planes are conjugate to each other and that bucket detectors are used in both arms.

Equation (3) can be rewritten in matrix form as $\mathbf{C} = \mathbf{AT}$, with $A_{mn} \equiv |A_m(-\mathbf{x}_n)|^2$ and $T_n \equiv |T(\mathbf{x}_n)|^2$. Most natural images are sparse when expressed in the proper basis such as that of the discrete cosine transform or the wavelet transform used in JPEG compression. Suppose the object intensity transmission function $\mathbf{T}$ is K-sparse in the basis $\boldsymbol{\Phi}$, i.e., only K of its coefficients are nonzero. When the measurement matrix $\mathbf{A}$ is taken to be a random matrix (such as a matrix whose entries are independent and identically Gaussian or Bernoulli distributed), it has been shown that the restricted isometry property (RIP) is satisfied [3,20,21]. Then according to the theory, the vector $\mathbf{T}$ gives the desired result by minimizing $\|\boldsymbol{\Phi}^T\mathbf{T}\|_1$ subject to the condition $\mathbf{C} = \mathbf{AT}$, in which $\|\mathbf{v}\|_1 = \sum_i |v_i|$ is the ℓ_1 norm of $\mathbf{v}$. The error in determining $\mathbf{T}$ is bounded from above if $M \gtrsim O[K\ln(N/K)]$ measurements are used. This number can be much smaller than that of the Nyquist-Shannon criterion, a number of order N.

Experiment. Our experimental setup is shown in Fig. 2. A continuous-wave Ar-ion laser (operating at a wavelength of 363.8 nm) was used to pump a BBO crystal cut for type-II collinear SPDC. The pump was spatially separated from the generated degenerate entangled photons using a prism. A polarizing beam splitter was used to send the orthogonally polarized photons into the object and reference arms. A phase-only reflective SLM (from Boulder Nonlinear: 512×512 pixels, pixel pitch 15 μm), sandwiched between orthogonal polarizers, was used to mimic an amplitude-only SLM. A half-wave plate was used to rotate the polarization of the photons before impinging on the SLM. The face of the nonlinear crystal is imaged using a lens (L in Fig. 2) of focal length $f = 25$ cm onto the object and the amplitude-only SLM
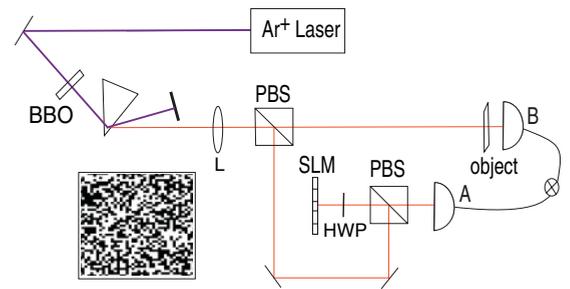

FIG. 2. (Color online) Setup for compressive quantum ghost imaging. PBS, polarizing beam splitter; SLM, spatial light modulator; L, imaging lens; HWP, half-wave plate; BBO, β-barium borate crystal. A and B represent bucket detectors used for coincidence measurement. Inset: example of a two-dimensional random binary pattern impressed onto the SLM.

with a magnification of 3. We group the native pixels of the SLM into cells with a size of 4×4 pixels, so that we effectively have an array with $N = 128 \times 128$ pixels. We then impress known but random binary patterns onto the SLM. We use identically distributed Bernoulli random variables (with values of 0 or 1) with equal probability. The photons transmitted through the optical system are coupled into a multimode fiber and registered by single-photon counting module (SPCM-AQR-14, from Perkin-Elmer) detectors in both arms. A 10-nm FWHM bandwidth spectral filter (centered at 727.6 nm) is placed in front of each detector. Coincidence circuitry (with a time window of 12 ns) was used to measure coincidence events between the avalanche photodiodes (APDs) in the reference and object arms.

We use two objects [the logo of the University of Rochester (UR), and the Greek letter Ψ] in the test arm of the ghost imaging setup, as shown in the insets of Figs. 3(a) and 3(b). A two-dimensional random binary amplitude mask (A_m) was sent to the SLM via a computer, and measurements were performed in coincidence (C_m) for $m = 1, \ldots, M$ where M is the total number of measurements. For each random pattern impressed onto the SLM, coincidence events were integrated for 9 s. On average, the singles counts in the object (reference) arms are 19.5×10^3 (25.6×10^3) counts/s for the logo and 28.3×10^3 (25.7×10^3) counts/s for Ψ. The coincidence rate is about $\sim 1\%$ of the singles rate.

To show the sparsity of the objects used in the experiment, we have used the two-dimensional discrete cosine transform (2D-DCT) as a representational basis. As can be seen in Figs. 3(c) and 3(d), the objects are sparse in the chosen basis (Φ).

The reconstruction of the object intensity transmission function ($\mathbf{T}$), was accomplished by minimizing $\|\Phi \mathbf{T}\|_{\ell_1}$ subject to $\mathbf{C} = \mathbf{AT}$ using the gradient projection algorithm [22]. The results of the reconstruction, for the maximum
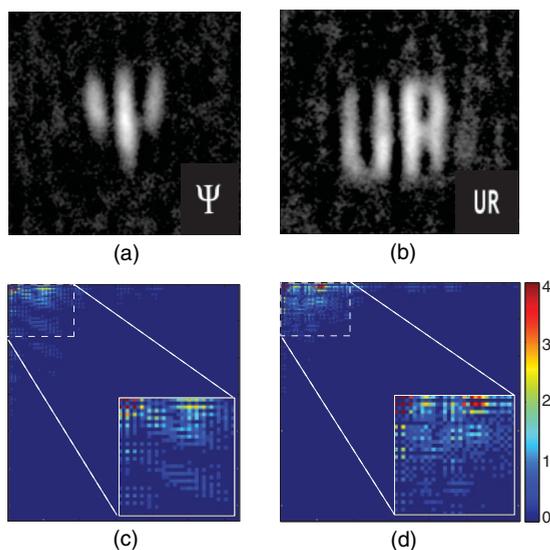

FIG. 3. (Color online) Reconstructed ghost image of (a) the Greek letter Ψ and (b) the UR logo. The insets show the masks used in the test arm of the ghost imaging setup. (c) and (d) The absolute value of the calculated two-dimensional discrete cosine transforms of the insets in (a) and (b), respectively.
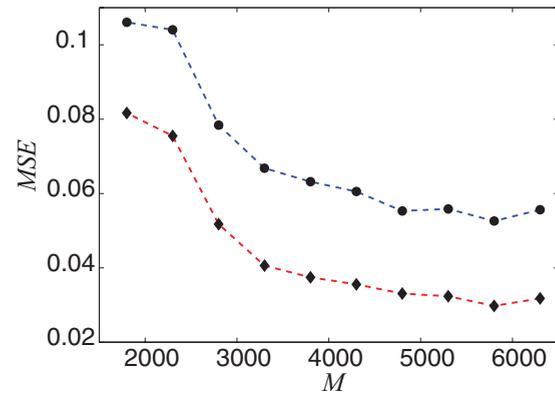

FIG. 4. (Color online) Calculated mean-squared error of the reconstructed ghost images of the UR logo ($\bullet$) and Ψ ($\blacklozenge$) as functions of the number of measurements M.

number of measurements ($M = 6300$), are shown in Figs. 3(a) and 3(b). Comparisons with the original masks of the objects (insets in the same figure) show that we have a good reconstruction.

To quantitatively characterize the fidelity of the CS image reconstruction, we use the mean-squared error (MSE) as our metric, where $\text{MSE} = (1/N) \|\hat{x} - x\|_2^2$. Here $\hat{x}$ is the reconstructed image, x represents the original mask, and N is the number of resolution cells, in our case $N = 128 \times 128$. Figure 4 shows the calculated MSE as a function of the number of measurements. As can be seen from the figure, the MSE flattens out for $M > 4500$ (27% of the Nyquist limit of 128×128), with values of 0.06 for the UR logo and 0.03 for the Greek letter Ψ.

We also characterize our CS results in terms of the signal-to-noise ratio (SNR). The signal and noise are calculated as the mean intensity of the bright pixels and the standard deviation of the dark background pixels, respectively [15]. The maximum SNR we obtained, for the maximum number of measurements $M = 6300$, is SNR = 8 (SNR = 10) for the object mask UR (Ψ) as shown in Fig. 5.

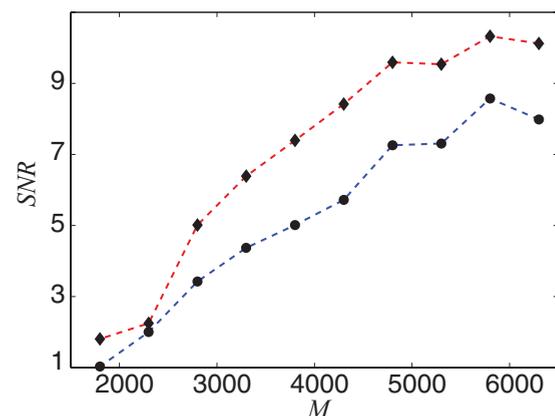Next, we compare the performance of our CS procedure with other approaches to image formation. For our

FIG. 5. (Color online) Calculated signal-to-noise ratio of the reconstructed ghost images of the UR logo ($\bullet$) and Ψ ($\blacklozenge$) as functions of the number of measurements M.

demonstrations, there are $128 \times 128 = 1.6 \times 10^4$ pixels in the object. We obtain a very good image using 6300 measurements (see Fig. 3) and a highly acceptable image using only 2000 measurements (see Fig. 5). Thus, we are able to obtain good images while performing far fewer measurements than there are pixels in the field to be imaged. We did not make any systematic attempt to minimize the total number of photons used to form the image. It is nonetheless interesting to examine the photon efficiency of our CS process. Using the numbers reported above, we estimate that approximately 1.4×10^7 detected biphotons were used to obtain either of the images of Fig. 3. This number is considerably smaller than the number required by conventional quantum ghost imaging, in which a point detector is raster scanned in the reference arm. In this case, we would need to collect approximately 100 photons per pixel to achieve a SNR of 10. There are 128×128 pixels in the image, but for raster scanning we utilize only 1 part in 128×128 of the emitted photons. Thus, the required number of photons is $100 \times 128^4 = 2.6 \times 10^{10}$.

In conclusion, we have experimentally demonstrated image reconstruction at low light levels using entangled photons from a SPDC source and using CS algorithms. We have shown that CS can lead to high-resolution images with a dramatically improved SNR. For the objects used in the experiment, high-fidelity ghost image reconstruction was achieved using only 27% of the number of measurements corresponding to the Nyquist limit. In addition, unlike most ghost imaging (quantum or thermal) experiments where spatially resolving detectors are a requirement, we used only single-pixel (bucket) detectors in both the reference and test arms. We believe this work will have an important impact in quantum imaging where photon counting arrays are an expensive and cumbersome resource and may have applications in secure image transmission [23] and optical encryption [24].

[1] E. Candès and T. Tao, IEEE Trans. Inf. Theory **52**, 5406 (2006).
[2] E. Candès *et al.*, Commun. Pure Appl. Math. **59**, 1207 (2006).
[3] D. Donoho, IEEE Trans. Inf. Theory **52**, 1289 (2006).
[4] D. Gross *et al.*, Phys. Rev. Lett. **105**, 150401 (2010).
[5] A. Shabani *et al.*, Phys. Rev. Lett. **106**, 100401 (2011).
[6] M. F. Duarte *et al.*, IEEE Signal Process. Mag. **25**, 83 (2008).
[7] J. H. Shapiro, Phys. Rev. A **78**, 061802(R) (2008).
[8] Y. Bromberg *et al.*, Phys. Rev. A **79**, 053840 (2009).
[9] T. B. Pittman *et al.*, Phys. Rev. A **52**, R3429 (1995).
[10] R. S. Bennink, S. J. Bentley, and R. W. Boyd, Phys. Rev. Lett. **89**, 113601 (2002).
[11] A. Valencia *et al.*, Phys. Rev. Lett. **94**, 063601 (2005).
[12] A. Gatti *et al.*, J. Mod. Opt. **53**, 739 (2006).
[13] F. Ferri *et al.*, Phys. Rev. Lett. **94**, 183602 (2005).
[14] R. Meyers, K. S. Deacon, and Y. Shih, Phys. Rev. A **77**, 041801 (2008).
[15] O. Katz *et al.*, Appl. Phys. Lett. **95**, 131110 (2009).
[16] L. Mandel and E. Wolf, *Optical Coherence and Quantum Optics* (Cambridge University Press, Cambridge, England, 1995).
[17] M. H. Rubin *et al.*, Phys. Rev. A **50**, 5122 (1994).
[18] R. S. Bennink *et al.*, Phys. Rev. Lett. **92**, 033601 (2004).
[19] A. F. Abouraddy *et al.*, Phys. Rev. Lett. **87**, 123602 (2001).
[20] R. G. Baraniuk *et al.*, Construct. Approx. **28**, 253 (2008).
[21] E. Candès and T. Tao, IEEE Trans. Inf. Theory **51**, 4203 (2005).
[22] M. A. T. Figueiredo *et al.*, IEEE J. Select. Topics Sig. Process. **1**, 586 (2007).
[23] M. Bondani *et al.*, J. Opt. Soc. Am. B. **25**, 1203 (2008).
[24] P. Clemente *et al.*, Opt. Lett. **35**, 2391 (2010).